Imaging Agents

DOI: 10.1002/ange.200604775

Development of a T_1 Contrast Agent for Magnetic Resonance Imaging Using MnO Nanoparticles**

Hyon Bin Na, Jung Hee Lee, Kwangjin An, Yong Il Park, Mihyun Park, In Su Lee, Do-Hyun Nam, Sung Tae Kim, Seung-Hoon Kim, Sang-Wook Kim, Keun-Ho Lim, Ki-Soo Kim, Sun-Ok Kim, and Taeghwan Hyeon**

Nanometer-sized colloidal particles (nanoparticles) have been extensively used in biomedical applications as a result of their many useful electronic, optical, and magnetic properties that are derived from their nanometer size and composition.[1] Semiconductor nanoparticles (also known as quantum dots) have been applied as fluorescent probes for cell labeling in optical imaging,[2] and gold nanoparticles derivatized with oligonucleotides have been used for sensing complementary DNA strands.[3] Magnetic nanoparticles have been applied to contrast-enhancement agents for magnetic resonance imaging (MRI), magnetic carriers for drug-delivery systems, biosensors, and bioseparation.[4]

MRI is one of the most powerful imaging techniques for living organisms as it provides images with excellent anatomical details based on soft-tissue contrast and functional information in a non-invasive and real-time monitoring manner.[5] MRI has further advanced by the development of contrast agents that enable more specific and clearer images and enlargements of detectable organs and systems, leading to a wide scope of applications of MRI not only for diagnostic radiology but also for therapeutic medicine. Current MRI contrast agents are in the form of either paramagnetic complexes or magnetic nanoparticles.[6] Paramagnetic complexes, which are usually gadolinium (Gd^{3+}) or manganese (Mn^{2+}) chelates, accelerate longitudinal (T_1) relaxation of water protons and exert bright contrast in regions where the complexes localize.[7] For instance, gadolinium diethylenetriaminepentaacetate (Gd-DTPA) has been the most widely used of such complexes and its main clinical applications are focused on detecting the breakage of the blood-brain barrier (BBB) and changes in vascularity, flow dynamics, and perfusion.[8] Manganese-enhanced MRI (MEMRI), which uses manganese ion (Mn^{2+}) as a T_1 contrast agent, is applicable to animals only owing to the toxicity of Mn^{2+} when it accumulates excessively in tissues and despite the increasing appreciation of this technique in neuroscience research.[9]

The recent development of molecular and cellular imaging to help visualize disease-specific biomarkers at the molecular and cellular levels has led to an increased interest in magnetic nanoparticles as MRI contrast agents. In particular, superparamagnetic iron oxide (SPIO) has emerged as the prevailing agent so far.[4,10] However, the negative contrast effect and magnetic susceptibility artifacts of iron oxide nanoparticles are significant drawbacks of using SPIO in MRI. The resulting dark signal can mislead the clinical diagnosis in T_2-weighted MRI because the signal is often confused with the signals from bleeding, calcification, or metal deposits, and the susceptibility artifacts distort the background image.[4b]

For the extensive applications of MRI to diagnostic radiology and therapeutic medicine and to overcome the

[*] Prof. J. H. Lee, Prof. S. T. Kim, Prof. S.-H. Kim
Department of Radiology, Samsung Medical Center
Sungkyunkwan University School of Medicine
Seoul 135-710 (Korea)
Fax: (+82) 2-3410-0084
E-mail: junghee42.lee@smc.samsung.co.kr

H. B. Na, K. An, Y. I. Park, M. Park, Prof. T. Hyeon
National Creative Research Initiative Center for Oxide Nanocrystalline Materials and School of Chemical and Biological Engineering
Seoul National University
Seoul 151-744 (Korea)
Fax: (+82) 2-886-8457
E-mail: thyeon@snu.ac.kr

Prof. I. S. Lee
Department of Chemistry and Advanced Material Science
Kyunghee University, Yongin 446-701 (Korea)

Prof. D.-H. Nam
Department of Neurosurgery, Samsung Medical Center
Sungkyunkwan University School of Medicine
Seoul 135-710 (Korea)

Prof. S.-W. Kim
Department of Molecular Science and Technology
Ajou University, Suwon 443-749 (Korea)

K.-H. Lim
NMR Laboratory, Asan Institutes for Life Science
University of Ulsan, Seoul 138-736 (Korea)

Prof. K.-S. Kim
Department of Pediatrics, Asan Medical Center
University of Ulsan, Seoul 138-736 (Korea)

Dr. S.-O. Kim
Biology and Clinical Pharmacology, Samyang R&D Center
Daejeon 305-717 (Korea)

[**] T.H. thanks the Korean Ministry of Science and Technology for financial support through the National Creative Research Initiative Program of the Korea Science and Engineering Foundation (KOSEF). J.H.L. was supported by the Center for Biological Modulators of the 21st Century Frontier R&D Program. We thank Sungman Jang and Heesouk Woo at the Samsung Medical Center for help in the MRI measurements and TEM studies. We thank Dr. Alan P. Koretsky at NINDS, NIH, and Dr. Seong-Gi Kim at the University of Pittsburgh for useful discussions. T_1 refers to the longitudinal relaxation time of water protons.

Supporting information for this article is available on the WWW under http://www.angewandte.org or from the author.

above-mentioned drawbacks of Gd^{3+}- and Mn^{2+}-based T_1 contrast agents and SPIO-based T_2 contrast agents, there has been great demand for a new class of contrast agent that satisfies the following characteristics: 1) positive (T_1) contrast ability, 2) intracellular uptake and accumulation for imaging cellular distribution and functions, 3) nanoparticulate form for easy surface modification and efficient labeling with targeting agents for applications in molecular and cellular imaging, and 4) favorable pharmacokinetics and dynamics for easy delivery, efficient distribution to biomarkers, and safe clearance from patients with minimal side effects. Here, we report the development of a long-awaited T_1 MRI contrast agent that satisfies all of these desirable characteristics using MnO nanoparticles.

Water-dispersible and biocompatible MnO nanoparticles were prepared according to a reported method with some modifications.[11,12] First, uniformly sized MnO nanoparticles (see Supporting Information) dispersed in nonpolar organic solvent were synthesized by the thermal decomposition of Mn-oleate complex.[11a] The particle size was controlled by varying either the solvent or reaction time. The resulting MnO nanoparticles dispersed in chloroform were then encapsulated in a polyethyleneglycol(PEG)-phospholipid shell to make them biocompatible.[12] Figure 1a shows the transmission electron microscopy (TEM) images of uniform and water-dispersed MnO nanoparticles of various sizes. They were highly crystalline and stable in water; they showed no degradation or aggregation in water over several months. They are antiferromagnetic (see Supporting Information), which means that they do not exert the susceptibility artifacts in MRI as observed with the SPIO-based T_2 agent.

To examine the possibility of using MnO nanoparticles as a MRI contrast agent, we measured relaxation times at a 3.0 T human clinical scanner of the size-tuned nanoparticles prepared in test tubes. As shown in Figure 1b, MnO nanoparticles with particle sizes of 7, 15, 20, and 25 nm at the same concentration of 5 mM (based on Mn concentration measured by inductively coupled plasma atomic emission spectroscopy (ICP-AES)) clearly showed bright signal enhancement in the T_1-weighted MRI, thus manifesting their potential applications as a T_1 contrast agent. The smaller the size of the nanoparticles, the brighter the signal is in the T_1-weighted MR image, which indicates that the T_1 shortening effect increases as the size of the nanoparticles decreases (Table 1). The MnO nanoparticles clearly decreased both the longitudinal relaxation time (T_1) and the transverse relaxation time (T_2).

To further investigate the contrast effect, we measured the specific relaxivities (r_1 or r_2) of the MnO nanoparticles. The

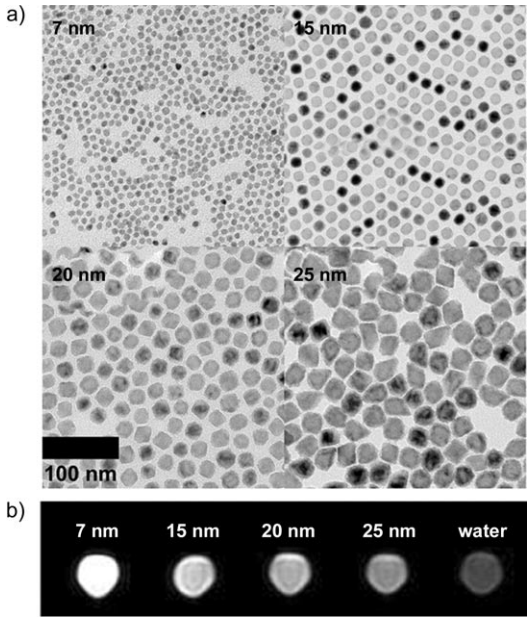

Figure 1. a) TEM images of water-dispersible MnO nanoparticles with particle sizes of 7, 15, 20, and 25 nm. b) T_1-weighted MR image of MnO nanoparticles from a 3.0 T clinical MRI system.

specific relaxivity (change in the relaxation rate per unit concentration of an agent, meaning "effectiveness" as a MRI contrast agent) is generally determined by measuring the relaxation rate as a function of concentration of the metal ions. We calculated the specific relaxivity (r_1) of the MnO nanoparticles with the different particle sizes (Table 1 and Supporting Information). Contrary to expectations, the r_1 value was found to be higher for the smaller MnO nanoparticles. Consequently, we defined another form of relaxivity ($r_{1(N)}$) based on the number of nanoparticles, given that the number of nanoparticles decreases as the size of the nanoparticles increases at the same metal content. The $r_{1(N)}$ value is higher for the larger MnO nanoparticles. Although the exact knowledge of the contrast-enhancement mechanism of MnO nanoparticles requires further investigation, we could speculate that the paramagnetic Mn^{2+} ions on the surface of the nanoparticles seem to be responsible for the shortening of the T_1 relaxation times. This hypothesis is further supported by the fact that another calculated relaxivity ($r_{1(S)}$) based on the total surface area of the nanoparticles is independent of the size of the nanoparticles. Furthermore, the r_1 value of the MnO/SiO_2 core–shell nanoparticles (see TEM image in the Supporting Information) was far lower than that of MnO

Table 1: Relaxation properties of the MnO nanoparticles.

Nanoparticle size [nm]	Longitudinal relaxation				Transversal relaxation			
	T_1[a] [ms]	r_1 [$mM^{-1}s^{-1}$]	$r_{1(N)}$ [$\mu M^{-1}s^{-1}$]	$r_{1(S)}$ [$m s^{-1}$]	T_2[a] [ms]	r_2 [$mM^{-1}s^{-1}$]	$r_{2(N)}$ [$\mu M^{-1}s^{-1}$]	$r_{2(S)}$ [$m s^{-1}$]
7	481	0.37	3	33	85	1.74	14	154
15	624	0.18	15	34	95	0.57	46	121
20	707	0.13	25	33	120	0.52	99	102
25	752	0.12	46	39	132	0.44	165	139

[a] The longitudinal (T_1) and transverse (T_2) relaxation times were measured at 5 mM Mn (as measured by ICP-AES).

nanoparticles, whereas the r_2 values of these two kinds of nanoparticles were nearly the same (see Supporting Information).

For in vivo MRI imaging, the 25 nm water-dispersible MnO nanoparticles (35 mg Mn (measured by ICP-AES) per kg of mouse body weight) were bolus-injected (rapid single shot) into a mouse through its tail vein. The body weights and possible changes in behavior of the animals were monitored for 3 weeks after the injection, and no signs of weight loss or abnormal behaviors were observed (see Supporting Information). The cytotoxicity of MnO nanoparticles was evaluated in eight human cell lines originating from various tissues. No appreciable toxicity was observed with a MnO concentration of less than 0.82 mM (based on the Mn concentration measured by ICP-AES) in human normal and cancer cell lines such as lung fibroblast, embryonic kidney, and glioblastoma cells or at a MnO concentration of 82 μM in hepatoma, large-cell lung cancer, breast adenocarcinoma, prostate adenocarcinoma, and leukemia cells (see Supporting Information).

Figure 2 shows the manganese oxide nanoparticle contrast-enhanced T_1-weighted MRI (designated as MONEMRI) of a mouse using the nanoparticles with a core size of 25 nm. In the T_1-weighted MONEMRI of the brain (Figure 2b and Supporting Information), the three orientations of the mouse brain show contrast-enhanced regions following accumulation of MnO nanoparticles in the tissues which were clearly observed in the TEM image of the cortex obtained 72 h after the injection (Figure 2f,g and Supporting Information). In comparison with non-contrast-enhanced images (Figure 2a), anatomic structures were clearly revealed in the brain. Interestingly, no appreciable contrast enhancement in T_2-weighted MRI was observed at the concentration of agent used in this study, despite the T_2 shortening effect in the in vitro measurement. The hippocampus structure, cortical layers, olfactory bulb layers, and cerebella gray matters (zoomed images in Figure 2c–f) are distinctively depicted in the MONEMRI. Such excellent brain MRI images that depict clear anatomic structures were previously only obtained using MEMRI, although a large dose of $MnCl_2$ was needed and injected slowly because of its low sensitivity and high toxicity.[9] This clear anatomic imaging of various brain structures suggests potential applications not only for basic neuroscience research but also for managing clinical neurological diseases such as neurodegenerative diseases, including Alzheimer's disease and Parkinson's disease, and other diseases that are accompanied by disturbances in neural cell structures without disturbing the blood brain barrier, including epilepsy and cortical dysplasia.

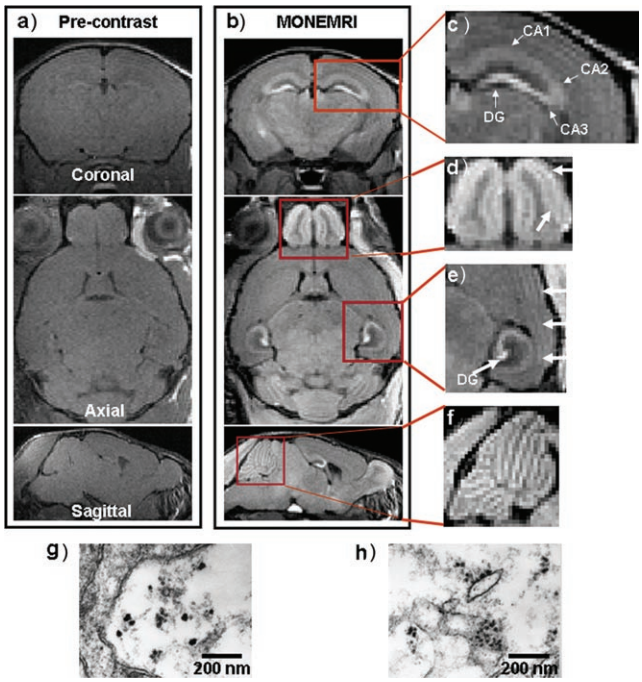

Figure 2. a, b) Typical coronal (top), axial (middle), and sagittal (bottom) views of a T_1-weighted 3D spin-echo MONEMRI before (a) and after (b) the administration of the MnO nanoparticles: the images in (b) show bright contrast enhancement in the brain structures owing to the accumulated MnO nanoparticles. c) The hippocampus structure is revealed showing the least-bright CA1, medium-bright CA2 and CA3, and the brightest dentate gyrus (DG). d) Axial view of the mouse olfactory bulb, showing the layers in the olfactory bulb. e) The ammon head of dentate gyrus is clearly shown, and the cortical layers are visible. f) The cerebellum structure is clearly visible, and the gray matters are enhanced. g, h) TEM images of the tissues taken from the cortex (g) and the hippocampus (h) show the presence of the MnO nanoparticles in the brain tissue.

The fine anatomic structures of the renal pelvis, medullar, and cortex were clearly revealed in kidney and the liver parenchyma, thus indicating the intracellular uptake of the nanoparticles in these organs as is supported by the TEM images (Figures S6 and S8 in the Supporting Information). The gray matter of the spinal cord was also clearly enhanced, a task that is very challenging in diagnostic radiology for managing neurodegenerative diseases.

For the selective imaging of disease-specific biomarkers in brain disease, in which T_1 contrast agents will certainly outperform SPIO-based T_2 contrast agents, we prepared functionalized MnO nanoparticles by conjugating them with *Her-2/neu* receptor antibody (Herceptin, Roche Pharma Ltd.) to selectively target the epidermal growth factor receptors (EGFRs) that are expressed at the cell surfaces of breast cancer. Figure 3a shows a series of MRI images of mouse brain bearing the breast cancer brain metastatic tumor that was intravenously injected with the Herceptin-functionalized MnO nanoparticles. The breast cancer cells were selectively enhanced in T_1-weighted MRI because the functionalized MnO nanoparticles with the EGFR-specific antibody were delivered and accumulated at the EGFR of the cell surface of the breast cancer. As the blood brain barrier is destructed as a result of the tumor formation in this animal model, both the functionalized and nonfunctionalized MnO nanoparticles entered the tumor site initially but only the functionalized MnO accumulate at the tumor site for an extended time owing to the presence of the conjugated antibody. As shown in Figure 3b, the nonfunctionalized MnO nanoparticles enhanced both the tumor and the normal brain tissues. To be used as a contrast agent in the brain, a prerequisite of a potential agent is clear marginal detectability without destroying anatomic background. A clear marginal detect-

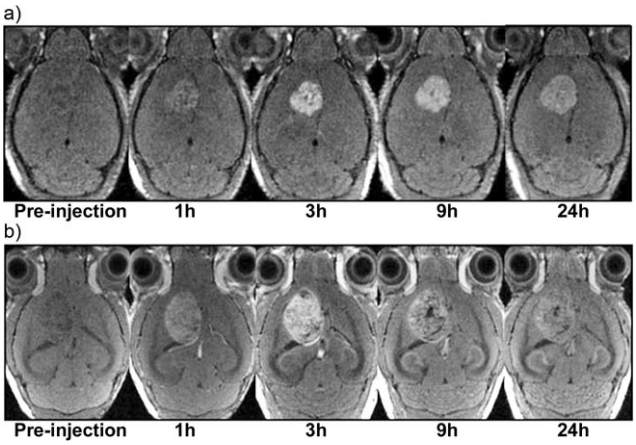

Figure 3. a) Breast cancer cells were selectively enhanced in T_1-weighted MRI because the Herceptin-functionalized MnO nanoparticles were delivered and accumulated at the EGFR at the surfaces of the breast cancer cells. b) The nonfunctionalized MnO nanoparticles enhanced both the tumor and the normal brain tissue.

ability with preserved anatomic background images was observed using the MnO nanoparticles, which is a remarkable advantage over SPIO and suggests the use of MnO nanoparticles for treating brain diseases.

In summary, we have reported the first biocompatible nanoparticulate T_1 MRI contrast agent for various body organs. We obtained clear T_1-weighted MR images of the brain, liver, kidney, and spinal cord from 5 days to 3 weeks after the administration of MnO nanoparticles which depicted fine anatomic structures. Furthermore, we have shown here that functionalized MnO nanoparticles prepared by conjugation with a tumor-specific antibody can also be used for selectively imaging breast cancer cells in the metastatic brain tumor. Easy delivery, clearance from the body organs and tissues, and a tolerable cellular toxicity range give us hope to develop this agent for future human clinical application as well. This new class of MRI contrast agent will open up a new direction in the applications of MR imaging for biomedical research and targeted therapy using molecular and cellular imaging in future medicine.

Received: November 24, 2006
Revised: January 19, 2007
Published online: March 13, 2007

Keywords: contrast agents · imaging agents · magnetic resonance imaging · manganese · nanoparticles

[1] a) C. M. Niemeyer, C. A. Mirkin, *Nanobiotechnology: Concepts, Applications and Perspectives*, Wiley-VCH, Weinheim, **2004**; b) A. P. Alivisatos, *Nat. Biotechnol.* **2004**, *22*, 47; c) K. J. Klabunde, *Nanoscale Materials in Chemistry*, Wiley-Interscience, New York, **2001**; d) T. Hyeon, *Chem. Commun.* **2003**, 927; e) J. Wang, *Small* **2005**, *1*, 1036; f) N. L. Rosi, C. A. Mirkin, *Chem. Rev.* **2005**, *105*, 1547; g) C. M. Niemeyer, *Angew. Chem.* **2001**, *113*, 4254; *Angew. Chem. Int. Ed.* **2001**, *40*, 4128.

[2] a) M. Bruchez, Jr., M. Moronne, P. Gin, S. Weiss, A. P. Alivisatos, *Science* **1998**, *281*, 2013; b) W. C. W. Chan, S. Nie, *Science* **1998**, *281*, 2016; c) S. Kim, Y. T. Lim, E. G. Soltesz, A. M. De Grand, J. Lee, A. Nakayama, J. A. Parker, T. Mihaljevic, R. G. Laurence, D. M. Dor, L. H. Cohn, M. G. Bawendi, J. V. Frangioni, *Nat. Biotechnol.* **2004**, *22*, 93; d) K. E. Sapsford, L. Berti, I. L. Medintz, *Angew. Chem.* **2006**, *118*, 4676; *Angew. Chem. Int. Ed.* **2006**, *45*, 4562; e) I. L. Medintz, H. T. Uyeda, E. R. Goldman, H. Mattoussi, *Nat. Mater.* **2005**, *4*, 435; f) X. Michalet, F. F. Pinaud, L. A. Bentolila, J. M. Tsay, S. Doose, J. J. Li, G. Sundaresan, A. M. Wu, S. S. Gambhir, S. Weiss, *Science* **2005**, *307*, 538; g) J. M. Klostranec, W. C. W. Chan, *Adv. Mater.* **2006**, *18*, 1953; h) X. Gao, Y. Cui, R. M. Levenson, L. W. K. Chung, S. Nie, *Nat. Biotechnol.* **2004**, *22*, 969; i) H. Mattoussi, J. M. Mauro, E. R. Goldman, G. P. Anderson, V. C. Sundar, F. V. Mikulec, M. G. Bawendi, *J. Am. Chem. Soc.* **2000**, *122*, 12142; j) I. L. Medintz, A. R. Clapp, J. S. Melinger, J. R. Deschamps, H. Mattoussi, *Adv. Mater.* **2005**, *17*, 2450; k) L. Medintz, A. R. Clapp, H. Mattoussi, E. R. Goldman, B. Fisher, J. M. Mauro, *Nat. Mater.* **2003**, *2*, 630; l) E. B. Voura, J. K. Jaiswal, H. Mattoussi, S. M. Simon, *Nat. Med.* **2004**, *10*, 993.

[3] a) T. A. Taton, C. A. Mirkin, R. L. Letsinger, *Science* **2000**, *289*, 1757; b) J.-M. Nam, C. S. Thaxton, C. A. Mirkin, *Science* **2003**, *301*, 1884; c) Y. W. C. Cao, R. Jin, C. A. Mirkin, *Science* **2002**, *297*, 1536; d) S.-J. Park, T. A. Taton, C. A. Mirkin, *Science* **2002**, *295*, 1503; e) M. S. Han, A. K. R. Lytton-Jean, B.-K. Oh, J. Heo, C. A. Mirkin, *Angew. Chem.* **2006**, *118*, 1839; *Angew. Chem. Int. Ed.* **2006**, *45*, 1807; f) P. Hazarika, B. Ceyhan, C. M. Niemeyer, *Small* **2005**, *1*, 844; g) C. M. Niemeyer, B. Ceyhan, P. Hazarika, *Angew. Chem.* **2003**, *115*, 5944; *Angew. Chem. Int. Ed.* **2003**, *42*, 5766; h) C. M. Niemeyer, B. Ceyhan, *Angew. Chem.* **2001**, *113*, 3798; *Angew. Chem. Int. Ed.* **2001**, *40*, 3685.

[4] a) R. Weissleder, K. Kelly, E. Y. Sun, T. Shtatland, L. Josephson, *Nat. Biotechnol.* **2005**, *23*, 1418; b) J. W. M. Bulte, D. L. Kraitchman, *NMR Biomed.* **2004**, *17*, 484; c) J. W. M. Bulte, S.-C. Zhang, P. van Gelderen, V. Herynek, E. K. Jordan, I. D. Duncan, J. A. Frank, *Proc. Natl. Acad. Sci. USA* **1999**, *96*, 15256; d) Y.-W. Jun, Y.-M. Huh, J.-S. Choi, J.-H. Lee, H.-T. Song, S. Kim, S. Yoon, K.-S. Kim, J.-S. Shin, J.-S. Suh, J. Cheon, *J. Am. Chem. Soc.* **2005**, *127*, 5732; e) H. Gu, P.-L. Ho, K. W. T. Tsang, L. Wang, B. Xu, *J. Am. Chem. Soc.* **2003**, *125*, 15702; f) C. Xu, K. Xu, H. Gu, X. Zhong, Z. Guo, R. Zheng, X. Zhang, B. Xu, *J. Am. Chem. Soc.* **2004**, *126*, 3392; g) J. Won, M. Kim, Y.-W. Yi, Y. H. Kim, N. Jung, T. K. Kim, *Science* **2005**, *309*, 121; h) C. Xu, K. Xu, H. Gu, R. Zheng, H. Liu, X. Zhang, Z. Guo, B. Xu, *J. Am. Chem. Soc.* **2004**, *126*, 9938; i) H. Gu, K. Xu, C. Xu, B. Xu, *Chem. Commun.* **2006**, 941; j) H.-T. Song, J.-S. Choi, Y.-M. Huh, S. Kim, Y.-W. Jun, J.-S. Suh, J. Cheon, *J. Am. Chem. Soc.* **2005**, *127*, 9992; k) Y.-M. Huh, Y.-W. Jun, H.-T. Song, S. Kim, J.-S. Choi, J.-H. Lee, S. Yoon, K.-S. Kim, J.-S. Shin, J.-S. Suh, J. Cheon, *J. Am. Chem. Soc.* **2005**, *127*, 12387; l) J.-H. Lee, Y.-W. Jun, S.-I. Yeon, J.-S. Shin, J. Cheon, *Angew. Chem.* **2006**, *118*, 8340; *Angew. Chem. Int. Ed.* **2006**, *45*, 8160; m) I. S. Lee, N. Lee, J. Park, B.-H. Kim, Y.-W. Yi, T. Kim, T. K. Kim, I. H. Lee, S. R. Paik, T. Hyeon, *J. Am. Chem. Soc.* **2006**, *128*, 10658; n) J. Kim, S. Park, J. E. Lee, S. M. Jin, J. H. Lee, I. S. Lee, I. Yang, J.-S. Kim, S. K. Kim, M.-H. Cho, T. Hyeon, *Angew. Chem.* **2006**, *118*, 7918; *Angew. Chem. Int. Ed.* **2006**, *45*, 7754; o) J. Kim, J. E. Lee, J. Lee, J. H. Yu, B. C. Kim, K. An, Y. Hwang, C. H. Shin, J. G. Park, J. Kim, T. Hyeon, *J. Am. Chem. Soc.* **2006**, *128*, 688.

[5] a) D. W. McRobbie, E. A. Moore, M. J. Graves, M. R. Prince, *MRI from Picture to Proton*, Cambridge University Press, Cambridge, **2002**; b) M. A. Brown, R. C. Semelka, *MRI: Basic Principles and Applications*, Wiley-Liss, New York, **2003**.

[6] U. Häfeli, W. Schütt, J. Teller, M. Zborowski, *Scientific and Clinical Applications of Magnetic Carriers*, Plenum, New York, **1997**.

[7] P. Caravan, J. J. Ellison, T. J. McMurry, R. B. Lauffer, *Chem. Rev.* **1999**, *99*, 2293.

[8] H.-J. Weinmann, W. Ebert, B. Misselwitz, H. Schmitt-Willich, *Eur. J. Radiol.* **2003**, *46*, 33.
[9] a) J. H. Lee, A. C. Silva, H. Merkle, A. P. Koretsky, *Magn. Reson. Med.* **2005**, *53*, 640; b) A. C. Silva, J. H. Lee, I. Aoki, A. P. Koretsky, *NMR Biomed.* **2004**, *17*, 532.
[10] a) A. S. Arbab, G. T. Yocum, H. Kalish, E. K. Jordan, S. A. Anderson, A. Y. Khakoo, E. J. Read, J. A. Frank, *Blood* **2004**, *104*, 1217; b) J. W. M. Bulte, T. Douglas, B. Witwer, S.-C. Zhang, E. Strable, B. K. Lewis, H. Zywicke, B. Miller, P. van Gelderen, B. M. Moskowitz, I. D. Duncan, J. A. Frank, *Nat. Biotechnol.* **2001**, *19*, 1141; c) M. G. Harisinghani, J. Barentsz, P. F. Hahn, W. M. Deserno, S. Tabatabaei, C. H. van de Kaa, J. de la Rosette, R. Weissleder, *N. Engl. J. Med.* **2003**, *348*, 2491.
[11] a) J. Park, K. An, Y. Hwang, J.-G. Park, H.-J. Noh, J.-Y. Kim, J.-H. Park, N.-M. Hwang, T. Hyeon, *Nat. Mater.* **2004**, *3*, 891; b) M. Yin, S. O'Brien, *J. Am. Chem. Soc.* **2003**, *125*, 10180; c) W. S. Seo, H. H. Jo, K. Lee, B. Kim, S. J. Oh, J. T. Park, *Angew. Chem.* **2004**, *116*, 1135; *Angew. Chem. Int. Ed.* **2004**, *43*, 1115; d) J. Park, E. Kang, C. J. Bae, J. G. Park, H. J. Noh, J. Y. Kim, J. H. Park, H. M. Park, T. Hyeon, *J. Phys. Chem. B* **2004**, *108*, 13598.
[12] B. Dubertret, P. Skourides, D. J. Norris, V. Noireaux, A. H. Brivanlou, A. Libchaber, *Science* **2002**, *298*, 1759.